Hydrogen Abstraction from Methane and Hydrofluoromethanes by •OH Radical: Modified GAUSSIAN-2 Study

Jacek Korchowiec,[†,‡] Shun-ichi Kawahara,[†] Kazunari Matsumura,[†] Tadafumi Uchimaru,*[,†] and Masaaki Sugie[†]

Department of Physical Chemistry, National Institute of Materials and Chemical Research, Agency of Industrial Science and Technology, MITI, Tsukuba Science City, Ibaraki 305-8565, Japan, and K. Gumiński Department of Theoretical Chemistry, Faculty of Chemistry, Jagiellonian University, R. Ingardena 3, 30-060 Cracow, Poland

Received: December 29, 1998; In Final Form: February 25, 1999

The reactions of methane and hydrofluoromethanes ($CH_{4-n}F_n$, $n = 0$, 1, 2, or 3) with a hydroxyl radical have been investigated by a modified GAUSSIAN-2 (G2M) method. Reaction enthalpies have been compared to those obtained by original G2 and G2MP2 schemes. The average absolute error for the reaction enthalpies calculated with the G2M method was smaller than those calculated with the G2 and G2MP2 schemes. G2M reaction enthalpies were of chemical accuracy. Moreover, the G2M method and selected MP2 schemes (those with the smallest average errors in the calculations for the reaction enthalpies) were used to compute the classical barrier heights. According to the transition state theory, the reaction rates were computed in the temperature range of 280−420 K and then the activation energies were obtained by the least-squares fitting to the Arrhenius equation. The activation energies calculated by using G2M barrier heights showed the best agreement with the experimentally derived values. The influence of the fluorine substitution effect on the activation energy was correctly described only by G2M barrier heights.

1. Introduction

Hydrofluorocarbons (HFCs) are possible replacements of fully halogenated chlorofluorocarbons (CFCs) which used to be widely applied as refrigerants, foam blowing substances, and aerosol spray propellants. Due to photolysis, the CFCs produce "ozone-consuming" chlorine atoms that result in ozone depletion in the stratosphere. The CFCs strongly influence the Chapman mechanism[1,2] for the creation and destruction of ozone in the stratosphere. On the other hand, the HFCs do not consume ozone in the stratosphere, since they do not contain chlorine atoms. However, the HFCs should have an impact on the radiative balance of the Earth. They are possible man-made sources of "greenhouse gases". Thus, the atmospheric lifetime of these compounds is an important measure of their environmental impact. To design environmentally friendly replacements of the CFCs, the atmospheric lifetime of the HFCs should be taken into account.

The essential role in the tropospheric chemistry is played by hydroxyl (•OH) radical.[1−3] The first step in degradation of the HFCs is hydrogen abstraction by •OH radical. The knowledge of the rate constants for the hydrogen abstraction reactions enables us to estimate the atmospheric lifetime of the HFCs. Thus, the kinetics and energetics of hydrogen abstraction from HFCs by •OH radical have been the subject of many experimental[3−7] and theoretical[8−14] investigations.

In the present study, we report theoretical investigations of hydrogen abstraction from methane and its fluoroderivatives by •OH radical:

$$CH_{4-n}F_n + {}^{\bullet}OH \rightarrow {}^{\bullet}CH_{3-n}F_n + H_2O \qquad (1)$$

where $n = 0$, 1, 2, or 3. Methane, the fluorine-free parent molecule, is one of the major components of natural greenhouse gases. Thus, all the reactions in eq 1 are of great importance in the atmospheric chemistry.

Among the four reactions, the system composed of •OH and CH_4 (•OH/CH_4) is the most extensively studied at different levels of theory,[13−22] since hydrogen abstraction from methane by •OH radical can be considered as a simple model for the key industry reactions of hydrocarbon combustion. Komornicki et al.[20] concluded that a correlation-consistent basis set and a high level of treatment of electron correlation [QCISD(T)] were required for adequate description of the kinetics and energetics for the system of •OH/CH_4. Truhlar et al.[18,19] applied Møller−Plesset (MP) perturbation theory to this system, scaling all correlation energy in second order (MP-SAC2). They pointed out the need of a large basis set for accurate description of the energy profile. Tyrrell et al.[12] reached a similar conclusion in their investigations on the •OH/CHF_3 system. Jursic[14] and Bottoni et al.[13] investigated all the reactions in eq 1. Jursic showed that density functional methods strongly underestimated activation energies.[14] Meanwhile, Bottoni et al. demonstrated that the activation energies were quite accurately described with an appropriate treatment of electron correlation. They optimized the geometries at the HF/3-21G(d) level and then applied the spin-projected second-order Møller−Plesset (MP2) perturbation theory with the 6-31G(d) basis set [PMP2/6−31(d)//HF/3-21(d)].[13] However, this level of theory failed to provide reasonable reaction enthalpies.

Our principal aim is to find a theoretical model that correctly describes the kinetics and energetics of hydrogen abstraction from HFCs by •OH radical. In this paper, we will show that a

* To whom correspondence should be addressed. Phone: +81-298-54-4522. Fax: +81-298-54-4487. E-mail: t_uchimaru@home.nimc.go.jp.
† National Institute of Materials and Chemical Research.
‡ Jagiellonian University.

10.1021/jp984810x CCC: $18.00
Published on Web 04/16/1999

computational method that combines high-level ab initio calculations with empirical correction is indispensable for accurate description of the energy profiles for the hydrogen abstraction reactions in eq 1. The results obtained with the computational methods, such as G2 (GAUSSIAN-2),[23] G2MP2[24] (G2 with basis set extension energy correction obtained at MP2 level), and G2M (modified GAUSSIAN-2)[25] schemes, will be mutually compared. Fluorine substitution effect for the reactions in eq 1 will be discussed as well.

2. Methods

We calculated the reaction enthalpies and the activation energies for the reactions in eq 1 by using the G2, G2MP2, and/or G2M schemes. The G2M calculations,[25] as well as G2[23] and G2MP2[24] calculations, were carried out according to the reported procedures (see also footnote to Table 1). The Gaussian 94 suite of programs[26] was employed on an IBM 6000.

In the G2 and G2MP2 schemes, the geometries were optimized at the Hartree−Fock (HF) and MP2 levels of theory with the 6-31G(d) basis set. The zero-point vibrational energies (ZPVEs) were calculated using the HF results with a scaling factor of 0.8929.[24] In the G2M scheme,[25] the geometries and ZPVEs (without scaling) were calculated using the hybrid density functional approach,[27] i.e., the Becke's three-parameter nonlocal exchange functional[28] with the nonlocal correlation functional of Lee, Yang, and Parr [B3LYP/6-311G(d,p)].[29,30] In contrast to the G2 or G2MP2 scheme, the G2M scheme of Morokuma et al.[24] additionally distinguishes the close- and open-shell systems via the projected MPn (PMPn) energies.[31] This should be especially important in free radical chemistry. The need of differentiating between close- and open-shell systems was also stressed by Radom et al.,[32,33] who introduced the CBS-RAD method for the treatment of free radicals. Among several G2M schemes,[25] G2M(cc, MP2) and G2M(rcc, MP2) schemes can be applied to relatively large systems. Thus, we chose these schemes for open- and closed-shell systems, respectively.

Activation energy is an experimentally derived quantity; it is defined as the slope of the Arrhenius plot, i.e.,

$$E_a \equiv -R \, \mathrm{dln} \; k(T)/\mathrm{d}(1/T) \tag{2}$$

where $k(T)$ is a rate constant, R is gas constant, and T is temperature. Frequently, the classical barrier height $\Delta E^{\ddagger}$ is compared with the experimental activation energy. The classical barrier heights for the reactions in eq 1 are given by

$$\Delta E^{\ddagger} = E_0^{\mathrm{TS}} - (E_0^{\bullet\mathrm{OH}} + E_0^{\mathrm{CH}_{4-n}\mathrm{F}_n}) \tag{3}$$

Here, E_0^{TS}, $E_0^{\bullet\mathrm{OH}}$, and $E_0^{\mathrm{CH}_{4-n}\mathrm{F}_n}$ are the energies (including ZPVEs) of the transition state, •OH radical, and methane (n = 0) or hydrofluoromethanes (n = 1, 2, 3), respectively.

According to the conventional transition-state theory (TST),[2,34] the rate constant $k(T)$ for the hydogen abstraction reactions is given as follows:

$$k(T) = \kappa \frac{k_b T}{h} \frac{Q^{\mathrm{TS}}}{Q^{\mathrm{OH}} Q^{\mathrm{CH}_{4-n}\mathrm{F}_n}} \exp(-\Delta E^{\ddagger}/RT) \tag{4}$$

where κ, Q, k_b, and h are transmission coefficient, partition functions, and Boltzmann's and Planck's constants, respectively. The activation energies reported for the hydrogen abstraction reactions in eq 1 were derived from the rate constants measured in the temperature region of 280−420 K. We calculated the rate constants in this temperature region using eq 4, and then the activation energies were derived by the least-squares fitting to the Arrhenius equation. Since partition functions are temperature dependent, the activation energy obtained from the fitting procedure should differ from the classical barrier height $\Delta E^{\ddagger}$.

We employed four models in order to compute the rate constatns $k(T)$. In all models, the Qs of transition states and reactants were approximated just as products of translational, rotational, vibrational, and electronic partition functions. In model I the electronic partition function is limited to the ground state, i.e., its degeneracy. In model II, we included additionally

TABLE 1: Reaction Enthalpies[a] for the Hydrogen Abstraction from Methane and Hydrofluoromethanes by •OH Radical at T = 298 K and P = 1 atm: $CH_{4-n}F_n + OH \rightarrow CH_{3-n}F_n + H_2O$ (n = 0, 1, 2, or 3)[b,f]

entry	method	$n=0$	$n=1$	$n=2$	$n=3$
A	MP2/6-31G(d)	−9.9	−14.0	−13.9	−8.8
	MP2/6-311G(d,p)	−12.9	−16.9	−16.6	−11.5
	MP2/6-311+G(d,p)	−16.1	−18.9	−18.6	−13.7
	MP2/6-311G(2df,p)	−13.6	−17.9	−17.9	−12.8
	MP2/6-311+G(3df,2p)	−17.6	−20.7	−20.5	−15.6
	MP4/6-311G(d,p)	−9.6	−13.4	−13.0	−7.8
	MP4/6-311+G(d,p)	−12.5	−15.3	−14.8	−9.8
	MP4/6-311G(2df,p)	−9.9	−14.0	−13.9	−8.8
	QCISD(T)/6-311G(d,p)	−9.4	−13.3	−12.8	−7.6
	G2[c]	−13.4	−16.5	−16.2	−11.2
	G2MP2[d]	−14.1	−17.1	−16.7	−11.7
B	B3LYP/6-311G(d,p)	−9.0	−14.5	−14.5	−9.3
	MP2/6-311G(d,p)	−12.9	−16.9	−16.6	−11.5
	MP2/6-311+G(3df,2p)	−17.5	−20.8	−20.5	−15.6
	PMP4/6-31G(d,p)	−7.3	−11.3	−11.1	−6.0
	PMP4/6-311G(d,p)	−9.7	−13.6	−12.8	−7.5
	CCSD(T)/6-31G(d,p)	−7.1	−11.1	−11.1	−6.1
	G2M[e]	−14.2	−17.5	−17.2	−12.4
	MP2/6-311+G(d,p)	−16.0	−19.0	−18.5	−13.6
	PMP2/6-311+G(d,p)	−16.1	−19.1	−18.2	−13.1
	MP2/6-311G(2df,p)	−13.5	−18.0	−17.9	−12.8
	PMP2/6-311G(2df,p)	−13.7	−18.1	−17.5	−12.3
	MP2/6-311G(3df,2p)	−14.9	−19.1	−19.1	−14.1
	PMP2/6-311G(3df,2p)	−15.1	−19.2	−18.7	−13.6
C	experimental values	−14.4	−19.3	−18.4	−12.2

[a] The reaction enthalpies at standard state (298 K, 1 atm) were computed as follows: $\Delta H = \Delta E_{\mathrm{el}} + \Delta E_{\mathrm{trans}} + \Delta E_{\mathrm{rot}} + \Delta E_{\mathrm{vib}} + P\Delta V$, where $\Delta E_X = E_X(H_2O) + E_X(CH_{3-n}F_n) - E_X(^{\bullet}OH) - E_X(CH_{4-n}F_n)$ and X corresponds to electronic (el), translational (trans), rotational (rot), or vibrational (vib) energy, respectively. [b] The experimental reaction enthalpies were obtained from standard enthalpies of formation. Data concerning methane, water, hydroxyl radical, and methyl radical were taken from ref 35. Standard enthalpies of formation for hydrofluoromethanes and hydrofluoromethyl radicals were taken from ref 37 and 38, respectively. [c] The G2 electronic energy is calculated as follows: E[G2] = E[MP4/6-311+G(d,p)] + E[MP4/6-311G(2df,p)] + E[MP2/6-311+G(3df,2p)] + E[MP2/6-311G(d,p)] + E[QCISD(T)/6-311G(d,p)] − 2E[MP4/6-311G(d,p)] − E[MP2/6-311+G(d,p)] − E[MP2/6-311G(2df,p)] + E(HLC), where $E(\mathrm{HLC}) = (4.81n_\beta - 0.19n_\alpha)/1000$ (in a.u.) is a higher level correction (HLC), n_β and n_α are the numbers of β and α valence electrons ($n_\alpha \geq n_\beta$). [d] The G2MP2 electronic energy is expressed as: E[G2MP2] = E[QCISD(T)/6-311G(d,p)] + E[MP2/6-311+G(3df,2p)] − E[MP2/6-311G(d,p)] + E(HLC); the HLC is exactly the same as for the G2 scheme. [e] In the G2M(cc, MP2) scheme, the electronic energy is as follows: E[G2M-(cc, MP2)] = E[PMP4/6-311G(d,p)] + E[MP2/6-311+G(3df,2p)] + E[CCSD(T)/6-31G(d,p)] − E[MP2/6-311G(d,p)] − E[PMP4/6-31G(d,p)] + E(HLC, cc, MP2), where $E(\mathrm{HLC,\ cc,\ MP2}) = (-5.05n_\beta - 0.19n_\alpha)/1000$. In the G2M(rcc, MP2) scheme, the restricted calculations are performed instead of unrestricted calculations and $E(\mathrm{HLC,\ rcc,\ MP2}) = (-4.93n_\beta - 0.19n_\alpha)/1000$. [f] The geometries of reactant and product were located at the MP2/6-31G(d) (entry A) and B3LYP/6-311(d, p) (entry B) levels of theory. The last entry (C) includes experimental values.

the low-lying excited state ($^2\Pi_{1/2}$) of •OH radical in the electronic partition function. The excitation energy of this state of •OH radical is 140 cm^{-1}.[35] The transition states for hydrogen abstraction reactions in eq 1 show a very low-frequency mode corresponding to the rotation of •OH radical fragment around the partially formed O−H bond. Thus, in model III, we employed the classical free rotor approximation rather than the quantum harmonic approximation for the very low-frequency modes. The last model IV, can be considered as a sum of models II and III. Namely, the low-lying excited state of •OH radical was taken into account and the free rotor approximation was employed. Furthermore, two cases were taken into account in all models. In the first case (a), the tunneling effect was neglected and the transmission coefficient κ was fixed to unity. Meanwhile, Wigner's tunneling correction[34]

$$\kappa(T) = 1 + h\nu^{\ddagger}/k_b T|^2/24 \qquad (5)$$

was employed in the second case (b). The calculated rate constants gave straight Arrhenius plots [$\ln k(T) = \ln A - E_a/RT$] for every case in models I−IV with the correlation coefficients higher than 0.999.

3. Results and Discussion

Table 1 shows the reaction enthalpies (ΔH), calculated at $T = 298$ K and $P = 1$ atm, for each reaction given in eq 1. Entry A gives G2 and G2MP2 predictions as well as the results obtained with the post-HF methods comprised in the G2 and G2MP2 schemes. Geometries optimized at the MP2/6-31G(d) level and the thermal corrections calculated at the HF/6-31(d) level of theory were employed. Meanwhile, entry B gives G2M reaction enthalpies and the results calculated at each computational level of the G2M scheme. The geometries and thermal corrections obtained at the B3LYP/6-311G(d,p) level were employed. In addition, the MP2/6-311+G(d,p), MP2/6-311G-(2df,p), and MP2/6-311G(3df,2p) predictions are given to estimate the effect of diffuse functions. In entry C, the reaction enthalpies obtained from the experimental values are reported. The geometrical parameters and energies of reactants and products are available as Supporting Information.

Table 2 reports the calculated classical barrier heights ($\Delta E^{\ddagger}$) and activation energies (E_a). All intermediate results (electronic energies and ZPVEs of transition-state structures) are available as Supporting Information. Entries A, B, and C show the values obtained at the computational levels of PMP2/6-311+G(d,p), PMP2/6-311G(2df,p), and PMP2/6-311G(3df,2p), respectively. The activation energies obtained from the spin unprojected MP2 energies are provided in parentheses. Entry D gives the corresponding values obtained with the G2M scheme. The experimentally measured activation energies are given in entry E. Transition-state structures located at the B3LYP/6-311G(d,p) level are shown in Figure 1. Moreover, the calculated activation energies (E_a) are plotted in Figure 2 as functions of the number of fluorine atoms in the substrates. The experimentally measured activation energies are also shown in the plots.

3.a. Reaction Enthalpies. All the hydrogen abstraction reactions in eq 1 are exothermic processes. The experimentally derived reaction enthalpies (entry C in Table 1)[35,37,38] range from −12.2 to −19.3 kcal/mol. All the reactions in eq 1 were predicted to be exothermic, regardless of the computational level utilized. However, most of the methods showed a tendency to predict less negative reaction enthalpies as compared with the experimental values; the exothermicity was underestimated (entries A and B in Table 1). The difference between the MP2/6-31G(d) and B3LYP/6-311(d,p) geometries is insignificant (see the Supporting Information). When the same computational methods were applied to these geometries, the calculated reaction enthalpies were very close to each other; the maximum deviation was not larger than 0.2 kcal/mol.

TABLE 2: Classical Barrier Heights $\Delta E^{\ddagger}$ and Activation Energies E_a (Models I−IV) for the Hydrogen Abstraction Reactions: $CH_{4-n}F_n + {}^{\bullet}OH \rightarrow {}^{\bullet}CH_{3-n}F_n + H_2O$ ($n = 0$, 1, 2, or 3)[b]

entry	quantity	$n = 0$	$n = 1$	$n = 2$	$n = 3$
A	$\Delta E^{\ddagger}$	5.3 (8.0)	4.7 (6.6)	5.2 (6.7)	6.7 (9.1)
	E_a (Ia)	5.7	5.2	5.9	7.6
	(Ib)	5.1	4.9	5.7	7.0
	(IIa)	5.6	5.1	5.7	7.5
	(IIb)	5.0	4.8	5.5	6.8
	(IIIa)	5.5	5.1	5.6	7.4
	(IIIb)	4.8	4.8	5.4	6.7
	(IVa)	5.3	4.9	5.5	7.2
	(IVb)	4.7	4.6	5.3	6.6
B	$\Delta E^{\ddagger}$	5.4 (8.6)	5.9 (8.3)	6.7 (8.9)	8.4 (11.7)
	E_a (Ia)	5.8	6.4	7.4	9.4
	(Ib)	5.2	6.1	7.2	8.7
	(IIa)	5.6	6.3	7.3	9.2
	(IIb)	5.0	6.0	7.1	8.5
	(IIIa)	5.5	6.2	7.2	9.1
	(IIIb)	4.9	5.9	7.0	8.4
	(IVa)	5.4	6.1	7.0	9.0
	(IVb)	4.7	5.8	6.8	8.3
C	$\Delta E^{\ddagger}$	4.5 (7.2)	4.3 (6.2)	4.7 (6.2)	6.2 (8.6)
	E_a (Ia)	4.9	4.9	5.4	7.1
	(Ib)	4.3	4.5	5.2	6.5
	(IIa)	4.8	4.7	5.3	7.0
	(IIb)	4.1	4.4	5.1	6.3
	(IIIa)	4.6	4.7	5.2	6.9
	(IIIb)	4.0	4.4	5.0	6.2
	(IVa)	4.5	4.5	5.0	6.8
	(IVb)	3.9	4.2	4.8	6.1
D	$\Delta E^{\ddagger}$	5.3	4.2	4.0	5.8
	E_a (Ia)	5.7	4.7	4.7	6.7
	(Ib)	5.1	4.4	4.5	6.0
	(IIa)	5.6	4.6	4.6	6.6
	(IIb)	5.0	4.3	4.4	5.9
	(IIIa)	5.5	4.5	4.5	6.5
	(IIIb)	4.8	4.2	4.3	5.8
	(IVa)	5.3	4.4	4.4	6.3
	(IVb)	4.7	4.1	4.1	5.6
E	E_a (exp)[a]	3.6	3.3	3.1	4.7

[a] Experimental values are taken from refs 4 and 5 and they are quite close to those reported in JPL-97 (*JPL Publications 97-4*; Jet Propulsion Laboratory, Calif. Inst. of Technology, 1997). [b] Entries A, B, C, and D correspond to the PMP2/6-311G(2df,p), PMP2/6-311+G(d,p), PMP2/6-311G(3df,2p), and G2M schemes, respectively. Values in parentheses are the unprojected barrier heights. Entry E summarizes the experimentally derived activation energies.

The reaction enthalpies calculated at the MP2/6-31G(d) and B3LYP/6-311G(d,p) levels of theory, which were employed in the geometry optimization in the G2 and G2M schemes, were highly less negative than the experimental values; the average deviations from the experimental values were +4.43 and +4.26 kcal/mol, respectively. For the post-HF calculations, the following tendencies were observed. First, MP4 calculations gave less negative reaction enthalpies as compared with the corresponding MP2 calculations. The reaction enthalpies calculated with the MP2 methods were closer to the experimental values than those calculated with the MP4 methods. Second, when polarization and diffuse functions were added to the basis set, the exothermicity increased. The effect of diffuse functions was greater than that of polarization functions. For both entries (A and B), the largest exothermicity, which is still larger than the experimental values, was predicted at the MP2/

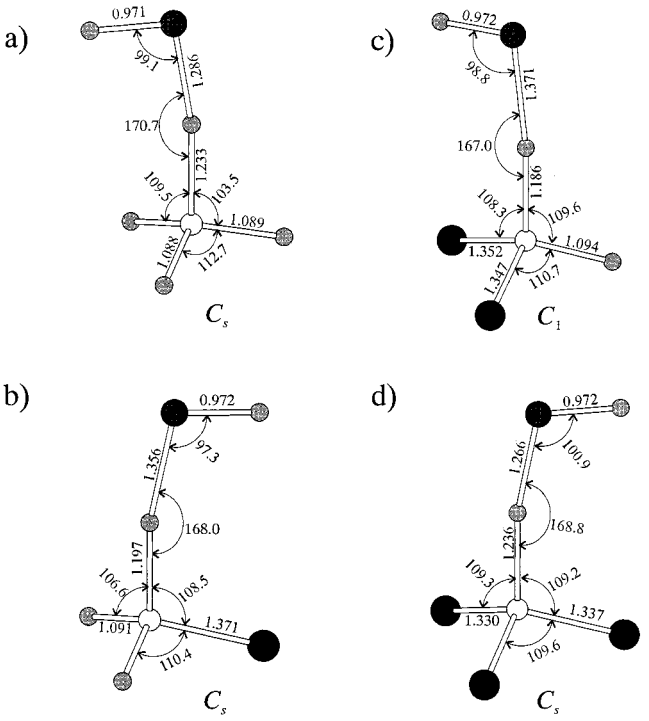

Figure 1. Perspective views of the transition-state structures, located at the B3LYP/6-311G(d,p) level of theory, corresponding to •OH/CH_4 (a), •OH/CH_3F (b), •OH/CH_2F_2 (c), and •OH/CHF_3 (d) systems. The bond lengths (Å) and selected angles (degrees) are also reported in the figure.

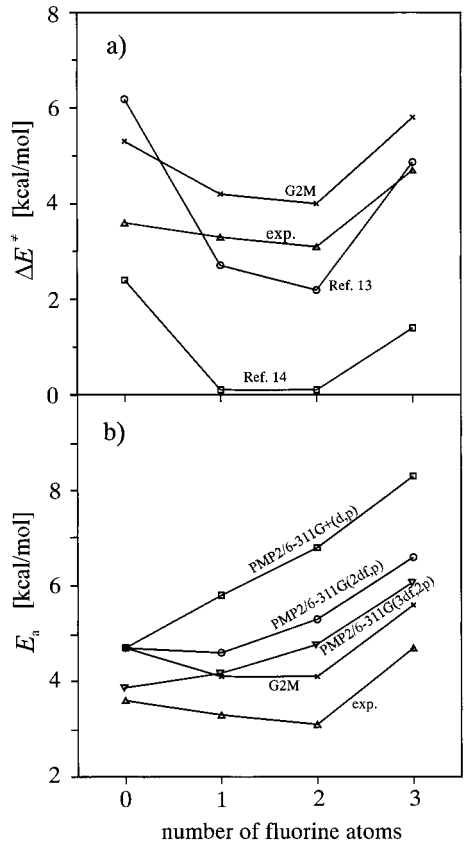

Figure 2. Dependence of the classical barrier height (part a) and activation energy (part b) on the number of fluorine atoms in the •OH/$CH_{4-n}F_n$ systems ($n = 0, 1, 2, 3$). In both parts, the experimentally measured activation energies are plotted as well.

6-311+G(3df,2p) level of theory using the largest basis set in the present work. Finally, the reaction enthalpies calculated from projected and unprojected energies were comparable to each other; the difference in the reaction enthalpies was less than 0.5 kcal/mol. Namely, the influence of spin contamination on the reactant and product energies was insignificant.

The experimentally derived reaction enthalpies indicate that the exothermicity of the hydrogen abstraction reactions increases in the following sequence: $-\Delta H$(•OH/CHF_3) < $-\Delta H$(•OH/CH_4) < $-\Delta H$(•OH/CH_2F_2) < $-\Delta H$(•OH/CH_3F). This trend was qualitatively reproduced in the calculated values of $-\Delta H$, regardless of the computational level utilized. Only in a few cases were the reaction enthalpies for •OH/CH_2F_2 and •OH/CH_3F systems comparable to each other in the unprojected calculations. Even in such cases, correct qualitative behavior was obtained after spin projection.

As seen in Table 1, MP2 calculations with a triple-ζ basis set (6-311G) and polarization/diffuse functions led to the reaction enthalpies relatively close to the experimental values. More specifically, the average absolute errors for the MP2/6-311+G(d,p), MP2/6-311G(2df,p), and MP2/6-311G(3df,2p) calculations in entry B were the smallest, 0.85, 0.82, and 0.82 kcal/mol for unprojected calculations, respectively, which were slightly reduced to 0.75, 0.72, and 0.72 kcal/mol after spin projection. The average absolute error for G2M reaction enthalpies was 0.85 kcal/mol, which is comparable to those for the MP2 calculations. The G2 and G2MP2 schemes gave slightly worse predictions; the average absolute errors were 1.75 and 1.17 kcal/mol, respectively.

3.b. Transition-State Geometries. The G2M scheme led to slightly better estimates of the reaction enthalpies than the G2 and G2MP2 schemes. Thus, we located the transition states at the B3LYP/6-311G(d,p) level of theory and then applied the G2M scheme to investigate the kinetics of the hydrogen abstraction reactions.

The optimized transition-state structures are shown in Figure 1. The transition-state structures for the •OH/CH_4, •OH/CH_3F, and •OH/CHF_3 systems had C_s symmetry and that for the •OH/CH_2F_2 system had C_1 symmetry. For the •OH/CH_4 system, the transition-state structure was in a staggered conformation, i.e., •OH radical and CH fragment of the methyl group, both located on the symmetry plane, were trans to each other. This transition-state structure is not in accord with those reported by Komornicki et al.,[20] Truhlar et al.,[18,19] and Gonzales et al.[15] They located the transition-state structures in the eclipsed conformation. In our calculations, however, the eclipsed conformation was found to be a second-order saddle point (two imaginary frequencies). The transition state in the staggered conformation was calculated to be lower in energy by only 0.02 kcal/mol than the saddle point in the eclipsed conformation. Meanwhile, the transition-state structures for •OH/CH_3F and •OH/CHF_3 systems were in the eclipsed conformation. The second-order saddle points had a staggered conformation for these systems. The F−C−O−H dihedral angle in the transition state for the •OH/CH_2F_2 system was close to zero. Thus, this transition-state geometry was considered to be in the eclipsed conformation.

According to Hammond's postulate,[39] a more exothermic reaction would take place through an earlier transition state. Thus, the transition-state structures for the hydrogen abstraction reactions in eq 1 would be more reactant-like rather than product-like. The lengths of the forming OH bond (r_{OH}) and breaking CH bond (r_{CH}) in the transition states can be used to characterize the transition states. Let us consider the following index:[16]

$$R = \{(r_{OH} - r_{OH}^{eq})/r_{OH}^{eq}\}/\{(r_{OH} - r_{OH}^{eq})/r_{OH}^{eq} + (r_{CH} - r_{CH}^{eq})/r_{CH}^{eq}\}$$

Distances r_{OH}^{eq} and r_{CH}^{eq} are the equilibrium bond lengths in water and methane (hydrofluoromethanes) molecules. The value of R was smaller than 0.5 for all the transition states, which suggests the reactant-like transition states in accord with Hammond's prediction. In addition, the value of R increases as follows: $^{\bullet}OH/CH_2F_2$ (0.17), $^{\bullet}OH/CH_3F$ (0.19), $^{\bullet}OH/CH_4$ (0.28), and $^{\bullet}OH/CHF_3$ (0.30). These values suggest that the transition states for the $^{\bullet}OH/CH_3F$ and $^{\bullet}OH/CH_2F_2$ systems would be significantly earlier than the transition states for $^{\bullet}OH/CH_4$ and $^{\bullet}OH/CHF_3$ systems. This implies that the fluorine substitution effects in $^{\bullet}OH/CH_{4-n}F_n$ systems cannot be interpreted as a simple additive rule. Moreover, the magnitude of R correlates with the exothermicity of the hydrogen abstraction reactions; the earlier transition states tend to result in the larger exothermicity. However, the value of R was slightly larger for $^{\bullet}OH/CH_3F$ than for $^{\bullet}OH/CH_2F_2$, although the former system is slightly more exothermic.

3.c. Classical Barrier Heights. We compared the classical barrier heights $\Delta E^{\ddagger}$ obtained from the G2M scheme (Table 2, entry D) with those calculated at the computational levels of PMP2/6-311+G(d,p), PMP2/6-311G(2df,p), and PMP2/6-311G-(3df,2p) (Table 2, entries A, B, and C), which gave the reaction enthalpies relatively close to the experimental values. The contamination of the wave functions for the transition states by higher spin states was much more significant as compared with those for the reactant and product radicals. The MP2 unprojected barrier heights, which are given in the parentheses in Table 2, were lowered by more than 1.5 kcal/mol after spin projection. Indeed, $\langle S^2 \rangle$ values (UHF level of theory) of the wave functions for transition states were ranging from 0.772 to 0.788, while for $^{\bullet}OH$ and $^{\bullet}CH_{3-n}F_n$ radicals $\langle S^2 \rangle$ did not exceed 0.762. The G2M scheme, which also employs the projected energies, gave still smaller barrier heights than the projected MP2 calculations. However, for the system of $^{\bullet}OH/CH_4$, the activation energies obtained in the G2M scheme were comparable to or slightly larger than the projected MP2 values.

The G2M barrier heights were closer to the experimentally derived activation energies as compared with those calculated with the projected MP2 schemes. Jursic[14] and Bottoni et al.[13] calculated the barrier heights for all the reactions in eq 1. We compared our G2M barrier heights with their results (Figure 2a). The barrier heights $\Delta E^{\ddagger}$ obtained with density functional calculations [B3LYP/6-11G(2d,2p)][14] are rather too low as compared with the experimentally measured activation energies. The PMP2/6-31(d)//HF/3-21(d) barrier heights[13] are closer to the experimental values. Our G2M barrier heights are slightly larger than the experimentally measured activation barriers. Importantly, the G2M barrier heights and the experimentally measured activation energies show parallel trends to each other with respect to the fluorine substitution in the substrate.

Aliagas and Gronert[22] applied the G2 and G2MP2 schemes for the $^{\bullet}OH/CH_4$ system; both schemes gave $\Delta E^{\ddagger} = 5.9$ kcal/mol. The same value of $\Delta E^{\ddagger}$ (5.9 kcal/mol) was obtained by Truhlar et al.[18,19] using the MP-SAC2 method. Meanwhile, Komornicki et al.[20] reported the value of 5.2 kcal/mol, which was obtained from the QCISD(T) calculations with the correlation-consistent basis set. Our G2M barrier height of 5.3 kcal/mol is slightly smaller than the values reported by Aliagas and Gronert and by Truhlar et al. but comparable to that reported by Komornicki et al. The $^{\bullet}OH/CHF_3$ system was investigated by Tyrrell et al.[12] The reported $\Delta E^{\ddagger}$ values of 7.8 and 9.6 kcal/mol for the PMP2/6-311G(d,p)//MP2/6-311G(d,p) and QCISD/6-311G(d,p)//MP2/6-311G(d,p) schemes, respectively, are significantly higher than our G2M value (5.8 kcal/mol).

3.d. Activation Energies. We computed the rate constants using the classical barrier heights obtained from the projected MP2 calculations and G2M scheme and then derived the activation energies by fitting to the Arrhenius equation. Going from model I to model IV (see Table 2), regardless of the computational levels utilized, the activation energies were gradually reduced. The activation energies E_a obtained in model I were larger than the corresponding classical barrier heights $\Delta E^{\ddagger}$. The more fluorine atoms in the substrates resulted in a greater difference between E_a and $\Delta E^{\ddagger}$. Inclusion of the low-lying excited state of $^{\bullet}OH$ radical into the electronic partition function (model II) showed a minor effect on the calculated activation energies; the values of E_a became smaller by about 0.1−0.2 kcal/mol. Slightly more pronounced lowering in the activation energy (0.1−0.3 kcal/mol) was seen when the free rotor approximation was used (model III). Finaly, in model IV, in which models II and III were combined, so due to additivity (logarithmic dependence in eq 2), the calculated activation energies were smaller by about 0.2−0.5 kcal/mol than those obtained from model I. The lowering of activation energy due to Wigner's correction was greater for the systems of $^{\bullet}OH/CH_4$ and $^{\bullet}OH/CHF_3$ than for those of $^{\bullet}OH/CH_3F$ and $^{\bullet}OH/CH_2F_2$.

Among models I−IV, model IV gave activation energies that were the closest to the experimentally derived values (see Table 2). In particular, the activation energies calculated from the G2M results using model IVb showed the best agreements with the experimental values (see Figure 2b); the average deviation from the experimental values was 0.95 kcal/mol. Even in this case, the activation energies were slightly overestimated. Except for the $^{\bullet}OH/CH_4$ system, the activation energies obtained in model IVb and the classical barrier heights calculated with G2M and the projected MP2 methods (see Table 2) were comparable to each other; the differences were of the order 0.1 kcal/mol. For the fluorine-free parent system ($^{\bullet}OH/CH_4$), the obtained activation energies were smaller by 0.6−0.7 kcal/mol than the calculated classical barrier heights.

The experimentally measured activation energy decreases smoothly on going from the $^{\bullet}OH/CH_4$ to $^{\bullet}OH/CH_2F_2$ system and then sharply increases and reaches the highest value for the $^{\bullet}OH/CHF_3$ system (Figure 2). The plots of the experimental activation energies and of G2M results in Figure 2b are almost parallel; the plot of G2M activation energies is shifted vertically about 1 kcal/mol above the experimental values. Thus, the activation energies obtained in the G2M scheme qualitatively reproduced the influence of fluorine substitution in the substrates on the activation energy. However, the similar trends were not observed for the projected MP2 activation energies; the projected MP2 calculations did not correctly reproduce the fluorine substitution effect.

The G2M scheme gave the best predictions of the activation energies for the hydrogen abstarction reactions in eq 1. Not only were the G2M activation energies closest to the experimentally measured values but also the influenec of fluorine substitution on the activation energies was correctly described by the G2M scheme.

4. Conclusions

In this paper, we have carried out systematic studies of the hydrogen abstraction from methane and from hydrofluoromethanes by $^{\bullet}OH$ radical. The reaction enthalpies were computed using the G2M, G2, and G2MP2 schemes. The

exothermicity of the hydrogen abstraction reactions increases in the following order: $-\Delta H(^{\bullet}OH/CHF_3) < -\Delta H(^{\bullet}OH/CH_4) < -\Delta H(^{\bullet}OH/CH_2F_2) < -\Delta H(^{\bullet}OH/CH_3F)$. Regardless of the computational levels utilized, including the post-HF methods comprised in the G2 and G2M schemes, the influence of fluorine substitution on the reaction enthalpies was correctly, at least qualitatively, described. The smallest average absolute errors (smaller than 1.0 kcal/mol) were found at PMP2/6-311G+(d,p), PMP2/6-311G(2df,p), and PMP2/6-311G(3df,2p) levels of theory. The average absolute error for the reaction enthalpies calculated with the G2M method was 0.85 kcal/mol, which is comparable to those for the PMP2 calculations. The average absolute errors in G2 and G2MP2 estimates of the reaction enthalpies were slightly larger.

For the activation energies, the values calculated with model IV were the closest to the experimentally derived values. In particular, the activation energies calculated with the G2M barrier heights using model IVb showed the best agreements with experimental values; the average deviation was 0.95 kcal/mol. In addition, the influence of fluorine substitution on the activation energies was correctly reproduced.

Thus, we can safely conclude that the modified GAUSSIAN-2 scheme of Morokuma et al. gives accurate reaction enthalpies and activation energies. The average absolute errors for both quantities were smaller than 1 kcal/mol.

Acknowledgment. J.K. greatly acknowledges support provided by STA Research Fellowship 296105. The services and computational time made available by the Computer Center in NIMC have been essential to this study and are gratefully acknowledged.

Supporting Information Available: Tables of (i) the optimized geometrical parameters of the reactants and products (supplementary Table 1S) and (ii) the absolute energies of the reactants, products, and transition states (supplementary Tables IIS−IVS). This material is available free of charge via the Internet at http://pubs.acs.org.

References and Notes

(1) Findlayson-Pitts, B.; Pitts, J. N. *Atmospheric Chemistry*; John Wiley: Chichester, 1986.
(2) Pilling, M. J.; Seakins, P. W. *Reaction Kinetics*; Oxford University Press: New York, 1995.
(3) Atkinson, R. *Chem. Rev.* **1985**, *85*, 69 and references therein.
(4) Hsu, K. J.; DeMore, W. B. *J. Phys. Chem.* **1995**, *99*, 1235.
(5) DeMore, W. B. *J. Phys. Chem.* **1996**, *100*, 5813.
(6) Orkin, V. L.; Huie, R. E.; Kurylo, M. J. *J. Phys. Chem. A* **1997**, *101*, 9118.
(7) Ravishankara, A. R.; Turnipseed, A. A.; Jensen. N. R.; Barone, S.; Mills, M.; Howard, C. J.; Solomon, S. *Science* **1994**, *263*, 71.
(8) Cooper, D. L.; Cunningham, T. P. *Atmos. Environ.* **1992**, *26A*, 1331.
(9) Martell, J. M.; Boyd, R. J. *J. Phys. Chem.* **1995**, *99*, 13402.
(10) Martell, J. M.; Tee, J. B.; Boyd, R. J. *Can. J. Chem.* **1996**, *74*, 786.
(11) Sekusak, S.; Gusten, H.; Sabljic, A. *J. Phys. Chem.* **1996**, *100*, 6212.
(12) Fu, Y.; Levis-Bevan, W.; Tyrrell, J. *J. Phys. Chem.* **1995**, *99*, 630.
(13) Bottoni, A.; Poggi, G.; Emmi, S. S. *THEOCHEM* **1993**, *279*, 299.
(14) Jursic, B. S. *Chem. Phys. Lett.* **1996**, *256*, 603.
(15) Gonzales, C.; McDouall, J. J. W.; Schlegel, H. B. *J. Phys. Chem.* **1990**, *94*, 7467.
(16) Truong, T. N.; Truhlar, D. G. *J. Chem. Phys.* **1990**, *93*, 1761.
(17) Jones, S. A. L.; Pacey, P. D. *J. Phys. Chem.* **1992**, *96*, 1764.
(18) Melissas, V. S.; Truhlar, D. G. *J. Chem. Phys.* **1993**, *99*, 1013.
(19) Melissas, V. S.; Truhlar, D. G. *J. Chem. Phys.* **1993**, *99*, 3542.
(20) Dobbs, K. D.; Dixon, D. A.; Komornicki, A. *J. Chem. Phys.* **1993**, *98*, 8852.
(21) Basch, H.; Hoz, S. *J. Phys. Chem. A* **1997**, *101*, 4416.
(22) Aliagas, I.; Gronert, S. *J. Phys. Chem. A* **1998**, *102*, 2609.
(23) Curtiss, L. A.; Raghavachari, K.; Trucks, G. W.; Pople, J. A. *J. Chem. Phys.* **1991**, *94*, 7221.
(24) Curtiss, L. A.; Raghavachari, K.; Pople, J. A. *J. Chem. Phys.* **1993**, *98*, 1293.
(25) Mebel, A. M.; Morokuma, K.; Lin, M. C. *J. Chem. Phys.* **1995**, *103*, 7414.
(26) Frisch, M. J.; Trucks, G. W.; Schlegel, H. B.; Gill, P. M. W.; Johnson, B. G.; Robb, M. A.; Cheeseman, J. R.; Keith, T.; Petersson, G. A.; Montgomery, J. A.; Raghavachari, K.; Al-Laham, M. A.; Zakrzewski, V. G.; Ortiz, J. V.; Foresman, J. B.; Cioslowski, J.; Stefanov, B. B.; Nanayakkara, A.; Challacombe, M.; Peng, C. Y.; Ayala, P. Y.; Chen, W.; Wong, M. W.; Andres, J. L.; Replogle, E. S.; Gomperts, R.; Martin, R. L.; Fox, D. J.; Binkley, J. S.; Defrees, D. J.; Baker, J.; Stewart, J. P.; Head-Gordon, M.; Gonzalez, C.; Pople, J. A. *Gaussian 94/DFT*, revision D.1; Gaussian, Inc.: Pittsburgh, PA, 1995.
(27) Becke, A. D. *J. Chem. Phys.* **1993**, *98*, 5648.
(28) Becke, A. D. *Phys. Rev. A* **1988**, *38*, 3098.
(29) Lee, C.; Yang, W.; Parr, R. G. *Phys. Rev. B* **1988**, *37*, 785.
(30) Miehlich, B.; Savin, A.; Stoll, H.; Preuss, H. *Chem. Phys. Lett.* **1989**, *157*, 200.
(31) Chen, W.; Schlegel, H. B. *J. Chem. Phys.* **1994**, *101*, 5957.
(32) Mayer, P. M.; Parkinson, C. J.; Smith, D. M.; Radom, L. *J. Chem. Phys.* **1998**, *108*, 604.
(33) Smith, D. M.; Nicolaides, A.; Golding, B. T.; Radom, L. *J. Am. Chem. Soc.* **1998**, *120*, 10223.
(34) Pacey, P. D. *J. Chem. Educ.* **1981**, *58*, 612 and references therein.
(35) Stull, D. R.; Prophet, H. JANAF Thermochemical Tables. *NSRDS-NBS* **1971**, *37*, 1.
(36) Wigner, E. *Z. Phys. Chem.* **1932**, *B19*, 203.
(37) Kolesov, V. P. *Russ. Chem. Rev.* **1978**, *47*, 599.
(38) McMillen, D. F.; Golden, D. M. *Annu. Rev. Phys. Chem.* **1982**, *33*, 493.
(39) Hammond, G. S. *J. Am. Chem. Soc.* **1953**, *77*, 334.